Journal of Applied Physics ARTICLE scitation.org/journal/jap

Characterizing the high-power-microwaves radiated by an axial output compact S-band A6 segmented magnetron fed by a split cathode and powered by a linear induction accelerator

Cite as: J. Appl. Phys. **133**, 133301 (2023); doi: 10.1063/5.0138769
Submitted: 14 December 2022 · Accepted: 18 March 2023 ·
Published Online: 5 April 2023

O. Belozerov,[1,a)] Ya. E. Krasik,[1] J. G. Leopold,[1] S. Pavlov,[1] Y. Hadas,[1] K. Kuchuk,[1] and E. Schamiloglu[2]

AFFILIATIONS

[1]Physics Department, Technion, Haifa 3200003, Israel
[2]Department of Electrical and Computer Engineering, University of New Mexico, Albuquerque, New Mexico 87131-0001, USA

[a)]**Author to whom correspondence should be addressed:** olegb@campus.technion.ac.il

ABSTRACT

In a recent publication [J. Appl. Phys. **131**, 023301 (2022)], microwave generation by a segmented A6 S-band axial output relativistic magnetron (RM) fed by a split cathode and powered by a small pulsed power generator was demonstrated for the first time. In the present article, we add to the same RM a mode converter and an antenna and drive it by using a modified linear induction accelerator (LIA) (≤450 kV, ≤4 kA, ∼150 ns). It was found that the operation of the RM for a split cathode or a common explosive emission cathode differs significantly. For a split cathode, we optimize for the best microwave output, its geometrical parameters, the external magnetic field, and the LIA's charging voltages. For the optimal choice of these parameters, the RM generates ∼160 ns long microwave pulses of ∼130 MW, 1.78 GHz frequency with an electronic efficiency of ∼40%, without pulse shortening. On the other hand, a common solid cathode fed RM showed microwave pulse shortening. We demonstrated that the segmented anode allows using a μs-timescale magnetic field, making it possible for the RM to operate repetitively.

I. INTRODUCTION

Extensive studies of relativistic magnetrons[1] (RMs) with radial or diffraction output show that this source can generate sub-μs-timescale high power microwave (HPM) pulses with power ≥1 GW and electronic efficiency as high as 70%.[2–4] However, the practical application of RMs is limited because of two major issues. First, pulse shortening, caused by the solid cathode's explosive plasma electron source, which expands toward the anode and can be unstable, leading to the termination of microwave generation at a time significantly earlier than the duration of the applied voltage.[2–5] To minimize the effects of this plasma on the operation of the RM, transparent cathodes[6] and different configurations with a virtual cathode[3,7–9] were tested. Whereas some of these concepts led to improvements over common solid explosive emission cathodes, neither of these approaches were completely successful because either the plasma is not removed when a transparent cathode is used or the proposed virtual cathode configurations were too difficult to implement.

The second issue has to do with the pulsed power system feeding the magnetic field producing solenoids. When the efficiency of an RM is considered, the power required to feed a solenoid or a Helmholtz coil to produce a few kG necessary for electron magnetization is neglected. However, if this power were to be considered, the effective efficiency of an RM system decreases drastically. This magnetic field needs to diffuse through the anode conducting material, which in most cases takes milliseconds. The latter requires the field producing system's power supply to store the energy of several kJ, making the weight and size of the system large and slow to charge, which impedes repetitive operation. The application of permanent magnets (see Refs. 10–12) makes a RM

more compact but the magnetic field cannot be varied. Smaller permanent magnets can be inserted in the cathode's inner volume and inside the vanes,[12] but then magnet edge effects interfere. When a large permanent magnet is used to produce a magnetic field along the entire RM structure, the system becomes large and heavy.[10]

Recently, we have verified solutions for these two problems in numerical simulations and experiments. We suggested to replace the explosive emission cathode with a split cathode, described in Refs. 13 and 14. A split cathode consists of an annular explosive plasma cathode placed a few cm upstream from the anode and connected by an axial metal rod to a circular electrode (a reflector) located a few cm downstream from the anode block. The plasma expansion velocities in the transverse direction and along directions enforced by the presence of magnetic fields of several kG are $\leq 10^6$[15,16] and $\leq 10^7$ cm/s, respectively.[15] Thus, the plasma remains outside the RM interaction space during several 100s ns. The electrons emitted from the plasma boundary are accelerated toward the anode and slow down near the reflector where they are reflected back upstream toward the cathode. Electrons oscillate between the cathode and the reflector, and their space charge screens the rod from explosive plasma formation. The electrons rotating in the azimuthal direction in the crossed electric and magnetic fields inside the anode interaction space serve as the source for the RM. In our first experiments,[17] a small pulsed power generator was used to power an axial output six-vane RM with either a split cathode or a solid cathode placed inside the anode interaction region. These experiments revealed that with the solid cathode, pulse shortening stops the HPM pulse, while the voltage pulse is still on, but it does not develop with a split cathode. Next, we suggested to use a RM with a segmented anode with thin gaps between segments, which allows almost simultaneous magnetic field penetration through the anode structure.[18] This design drastically decreases the required stored energy of the pulsed power source feeding the solenoid magnet. The experiments showed that the operation of a segmented RM is not affected by the presence of these gaps. A power source feeding the solenoid with a stored energy of ≤ 200 J was sufficient to produce a magnetic field of several kG over 90 μs, and ~200 ns, ~50 MW HPM pulses were generated.[19]

Recent research[20] showed that a diocotron instability can develop in the counterstreaming flow of electrons trapped in the longitudinal potential well between the two parts of the cathode. Moreover, numerical simulations revealed a complex interplay between the diocotron and RM modes, which influence the HPM pulse parameters and depend on the geometric parameters of the system and the magnetic field.[21]

In this article, we present the results of the experiments for the same RM as that described in Ref. 18 except with a mode converter and a conical antenna added; the resultant radiated HPM was characterized. In this research, the RM was powered by a modified linear induction accelerator (LIA). The split cathode is a very promising electron source for a RM, but its operation is based on an underlying complex and special electron dynamics.[20] Because of this, we performed the experiments in which the dependence of the HPM pulse parameters on the cathode–anode–reflector gaps, the emitter diameter, the anode length, and different values of the external magnetic field for different charging voltages of the LIA were scanned. As in our earlier work, we compare the split cathode's performance with that of a common solid explosive emission cathode.

The remainder of this article is organized as follows. In Sec. II, the LIA, its modifications, the experimental setup, and the diagnostic methods are described. The experimental results are presented in Sec. III, and in Sec. IV, our conclusions are summarized.

II. EXPERIMENTAL SETUP AND DIAGNOSTICS

The LIA,[3] developed at the Nuclear Research Institute, Tomsk, Russia, was used over ten years in our earlier research of an S-band RM[22–26] with excellent reliability and reproducibility. However, in a later research, there were indications that a major refurbishment was needed. During the LIA's refurbishment, the intermediate storing capacitor was replaced by six low-inductance 100 kV, 40 nF capacitors connected in parallel, and new pulse forming lines of the induction sections were manufactured. Tests of the refurbished LIA using a planar electron diode showed that it operates reliably with a voltage amplitude of ~450 kV, ~4 kA current, ~50 ns rise time, and pulse duration of ~150 ns FWHM (full width at half maximum).

This modified LIA was used in this research as the pulsed power source to drive the segmented anode RM fed by either a split cathode or a solid cathode installed inside the anode. The design of this RM was described in Ref. 19 with dimensions set by particle-in-cell (PIC) simulations (see Ref. 18), where the design of the solenoid and it power supply are also reported. For the reader's convenience and because of some variations in the geometrical dimensions of the anode and cathodes, we repeat this description.

The aluminum anode was either 40 or 60 mm long with 21/42 mm inner/outer anode radii, respectively. The anode is surrounded by a cylindrical tube followed by a closed conical section. The tube has radial slots so that all cavities are open [Fig. 1(a)]. Three vanes are continued axially, reaching the system's outer radius, making up a three-segment cylindrical structure that collects the microwave output and transmits it in the axial direction. Three 2 mm wide angular slits are cut radially at the center angle of three vanes [see Figs. 1(a) and 1(c)], the inner tube of the radiator and the outer tube. A tube at the outer RM radius continues downstream where it ends in a closed conical tube. The conical structure transforms the axial output to a TM_{01} waveguide mode. This axial output RM is placed inside a 400 mm long, 130 mm diameter Perspex tube [Figs. 1(a) and 1(c)], and a vacuum of 10^{-3} Pa is maintained using a turbo-molecular pump.

The TM_{01} waveguide mode formed at the downstream end of the axial output RM is the input to a mode converter based on a design proposed in Ref. 27 but changed to fit the parameters of our system to avoid vacuum breakdown. The mode converter transfers the circular TM_{01} mode to the TE_{11} mode required by the horn antenna attached at its end. The mode converter matches the two modes using four conductive posts and a conductive plate [see Fig. 1(a)]. The dimensions of these and the mode converter's tube profile were optimized for the best conversion efficiency using Ansys HFSS[28] simulations. The horn antenna is 50 cm-long with inner and outer diameters of 10 and 40 cm, respectively. These dimensions of the antenna correspond to a simulated directivity of ~17 dB.

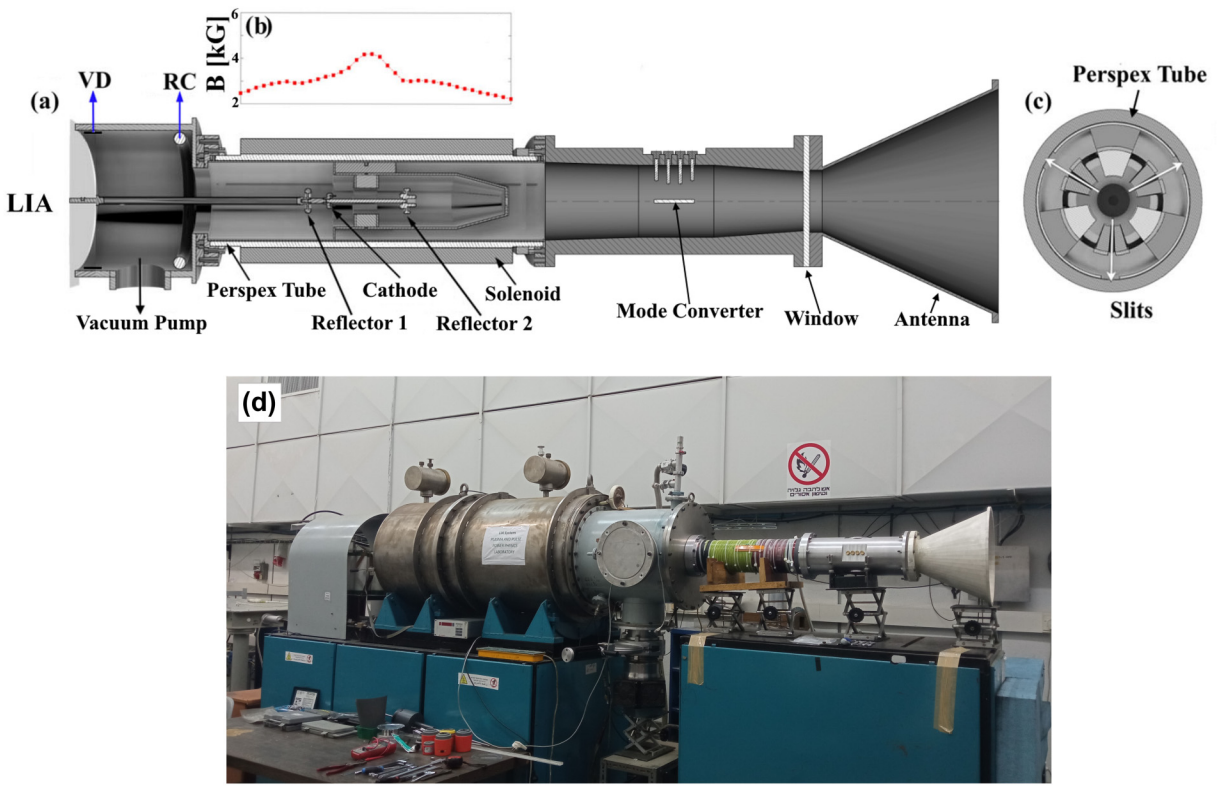

FIG. 1. Longitudinal cross section of the experimental setup (a) and the axial magnetic field distribution (b) for 4 kV charging voltage of the pulsed power supply. The white arrows in the azimuthal cross section at the magnetron center point out the position and extent of the three longitudinal slits (c). External view of the LIA with installed RM (d).

The emitter of the split cathode consists of 5 mm long, 1/0.75 mm outer/inner diameter tubes of carbon capillaries fixed in holes drilled in a 40 mm diameter cathode. The capillaries were symmetrically distributed along either 16 or 12 mm diameter circles. The axial distance between the upstream edge of the anode and the edge of the carbon capillaries was varied in the range 15–40 mm. The diameter of the rod connecting the emitter with the 40 mm diameter downstream reflector was either 6 or 9 mm. The axial distance between the reflector and downstream edge of the anode was varied in the range 15–40 mm to keep the emitter–anode and anode–reflector gaps the same. We denote these equal gaps below using the letter G. The cathode, rod, and reflector are hard coated with a 0.1 mm thick layer of aluminum oxide to suppress explosive plasma formation. The solid cathode, a 16 mm diameter carbon rod with 12 1 mm deep azimuthally distributed longitudinal grooves, was either 20 or 30 mm long.

The solenoid was built from a single wire layer wound around the Perspex tube. The solenoid is energized by a current pulse of 90 μs half-period, produced by the discharge of a 25 μF capacitor charged to a voltage ranging from 1.6–4.0 kV (stored energy $\leq$ 200 J), which produced a magnetic field ranging from 2 to 4 kG distributed axially [see Fig. 1(b)].

The current and voltage waveforms were measured by a self-integrating Rogowski coil (RC) and a capacitive voltage divider (VD), respectively, placed at the output of the LIA [see Fig. 1(a)]. The microwave electric field was measured by a D-dot sensor SFE-10G (Montena) with a PRODYN Balun BIB-100G (250 kHz–10 GHz) placed at a distance of 190 cm from the antenna. The electric field E (V/m) was calculated as $E = U_d 10^{k/20}/2\pi f \varepsilon_0 Z S$, where f is the microwave frequency, ε_0 is the dielectric constant of free space, $Z = 50\,\Omega$ is the impedance of the balun, $S = 2 \times 10^{-4}$ m^2 is the cross-sectional area of the D-dot dipole, U_d is the peak voltage of the microwave signal registered by the digitizing oscilloscope, and k is the total attenuation coefficient in dB, which includes the balun attenuation of 8 dB, the cable attenuation of 21 dB, and the attenuators placed at the input of the Agilent Infinium DSO 81204B digitizing oscilloscope (12 GHz, 20 GSa/s), which recorded the signals. The spatial distribution of the microwave power in the horizontal or vertical polarization of the D-dot sensor was measured at a distance of 190 cm from the output window or antenna, which can be considered as in the far-field for microwaves of ~2 GHz frequency. At least, five shots were performed for each set of parameters when measuring microwaves.

III. EXPERIMENTAL RESULTS

A. Operation of the RM with a split cathode

HPM generation in a split cathode fed RM was studied for different values of the LIA charging voltages, $\varphi_{ch} = 1.7–2.6$ kV, magnetic fields, $B_z = 0.2–0.4$ T, and RM geometrical parameters. Here, let us note that for a matched load of 100 Ω, when the charging voltage of the primary stored capacitor of the LIA is varies in the range 1.7–2.6 kV, the output voltage varies approximately in the range 260–400 kV. However, the applied voltage amplitude strongly depends on the RM impedance, that is, on the value of the magnetic field and the magnetron geometry.

Preliminary measurements of the HPM pulse parameters at a distance of 190 cm from the output of the antenna but without a mode converter and an antenna revealed that the RM generates microwaves with radial polarization as one should expect for the TM_{01} mode. Adding the mode converter and antenna led to the transformation of the TM_{01} mode to the TE_{11} mode, but the total power of the HPM pulse decreased to almost half. The total power was calculated using the measured spatial distribution of the HPM electric field on a plane at a distance of 190 cm from the antenna (see below). At this point, we do not know the reason for this, but we plan to perform additional simulations to understand and improve the efficiency of the system. Because of this problem, the RM with split cathode was tested with the antenna attached directly to the axial output of the RM without the mode converter (see Fig. 1).

The generation of microwaves starts at a magnetic field as low as ∼0.23 T for the entire range of φ_{ch} values, but the generated microwave power does not exceed ∼30 MW and the time delay between the onset of the voltage and the start of the microwave generation was very long ($\tau_d \sim 150$ ns). The onset time of the LIA voltage is defined at 10% of its maximal amplitude. As the magnetic field is increased above 0.27 T, the microwave power increases considerably. For the split cathode fed RM, we do not compare the magnetic field with the Hull magnetic field value because the electrons oscillating inside the anode have a potential energy smaller than the cathode potential. Because of this, the magnetic field necessary for electron magnetization is smaller than that required by the Hull criterion applied for the case of a cathode located inside the anode.

Typical waveforms of the voltage, φ_{RM} (the voltage supplied to the RM by a LIA charging voltage of φ_{ch}), current I_{RM}, and the microwave electric field of vertical polarization measured by the D-dot probe placed on the axis at a distance of 190 cm from the output of the antenna and time-frequency analysis of the latter are shown in Fig. 2. The voltage pulse rises to ∼300 kV, but as the RM current increases, it drops to ∼150 kV because of LIA-RM impedance mismatch. These waveforms were obtained for a 60 mm long anode, 11.5 mm diameter cathode emitter, 6 mm diameter rod, $G = 15$ mm, $B_z = 0.32$ T, and $\varphi_{ch} = 2.6$ kV. One can see in Fig. 2(a) that there is a ∼10 ns time delay in the beginning of the current, which can be related to the electric field threshold of ∼20 kV/cm, which is necessary for the formation of explosive emission plasma at the edges of the carbon capillaries. Also, one can see that the vertically polarized microwave generation starts with a time delay of $\tau_d \approx 45$ ns when the amplitude of the current reaches $I_{RM} = 0.8$ kA and it continues ∼160 ns. In the horizontal polarization, the microwave generation starts with the same τ_d, but it is slightly shorter (∼125 ns). The microwave electric fields were almost equal for both polarizations, and the microwave frequency f = 1.78 GHz [Fig. 2(c)] is the same during the entire HPM pulse generation.

Figure 3(a) displays the spatial distribution of the HPM pulse's total power density for the RM for the same parameters as used in Fig. 2. This distribution was obtained by the D-dot probe measuring the electric field in 10° steps along a horizontal semicircle on a virtual plane at a 190 cm distance from the antenna exit. Using this distribution, the directivity of the antenna was determined as $D_{dB} = 10\log(41253/1.64\Omega_{1d}\Omega_{2d}) \approx 17$ dB, which agrees well with the calculated value of directivity. Here, it was considered that $\Omega_{1d} \approx \Omega_{2d} \approx 20°$ are the half-power beam widths in the vertical and horizontal planes. The D-dot measurements show that the spatial distributions for the vertical and horizontal polarizations are the same. Considering that the power flux density is related to the electric field as $E(\mathrm{V/cm}) = 19\sqrt{P(\mathrm{W/cm^2})}$,[29] and the total power density was calculated as the sum of the power densities for each electric field polarization. Then, the total radiated instantaneous power, $P_{MW} \approx 130$ MW, is calculated assuming the azimuthal uniformity of the measured distribution of the electric field in the meridian plane. This power corresponds to electronic efficiency $\eta = (P_{MW}/P_{LIA}) \times 100\% \approx 40\%$, where $P_{LIA} = \varphi_{LIA} \times I_{RM}$ at the maximal measured electric field. For comparison, in Fig. 3(b), one can see the spatial distribution of the total power density obtained without the antenna at a distance of 190 cm from the output window of the RM tube. In this case, as expected, a rather broad spatial distribution of the microwave power density was obtained and whose integration results in the same total radiated power as that calculated using the data in Fig. 3(a).

As mentioned above, the Hull condition is difficult to determine for the split cathode fed RM. Nevertheless, the Hull and Buneman–Hartree limits should exist for a split cathode fed RM as well. That is, there must be a lower bound to the magnetic field for minimal magnetic insulation and an upper bound too where the best synchronization exists between the electron azimuthal drift and electromagnetic wave phase velocities. However, the formulas developed for both these limits for ordinary cathode fed RMs are not applicable to a split cathode fed device. Thus, the experiments were carried out for magnetic fields in the range 0.23–0.4 T. It was found that the time delay τ_d between HPM pulse duration and the total power is affected very strongly by the value of the applied magnetic field. In Fig. 4, these dependencies are shown for $G = 30$ mm, 11.5 mm diameter cathode emitter, 60 mm long anode, and a 6 mm diameter rod. One can see that the time delay decreases to $\tau_d \approx 45$ ns with increasing magnetic field until $B_z = 0.35$ T. The reason for this could be faster electron space charge accumulation in the anode interaction space for the stronger magnetic field, which leads to the earlier start of the microwave generation as well as to a complex synchronization between the RM mode's frequency, the azimuthally drifting electron spokes, and the longitudinally oscillating electron charge, which also depends on the value of the external magnetic field.[20] The HPM pulse duration first increases with increasing magnetic field due to the decrease in τ_d, but for $B_z > 0.28$ T, the pulse duration decreases [see Fig. 4(b)]. The duration of the longest HPM pulse reached ∼170 ns, as long as the corresponding applied voltage pulse. Figure 4(b) also shows that the HPM power increases with magnetic field up to $B = 0.32$ T, above which it is almost constant.

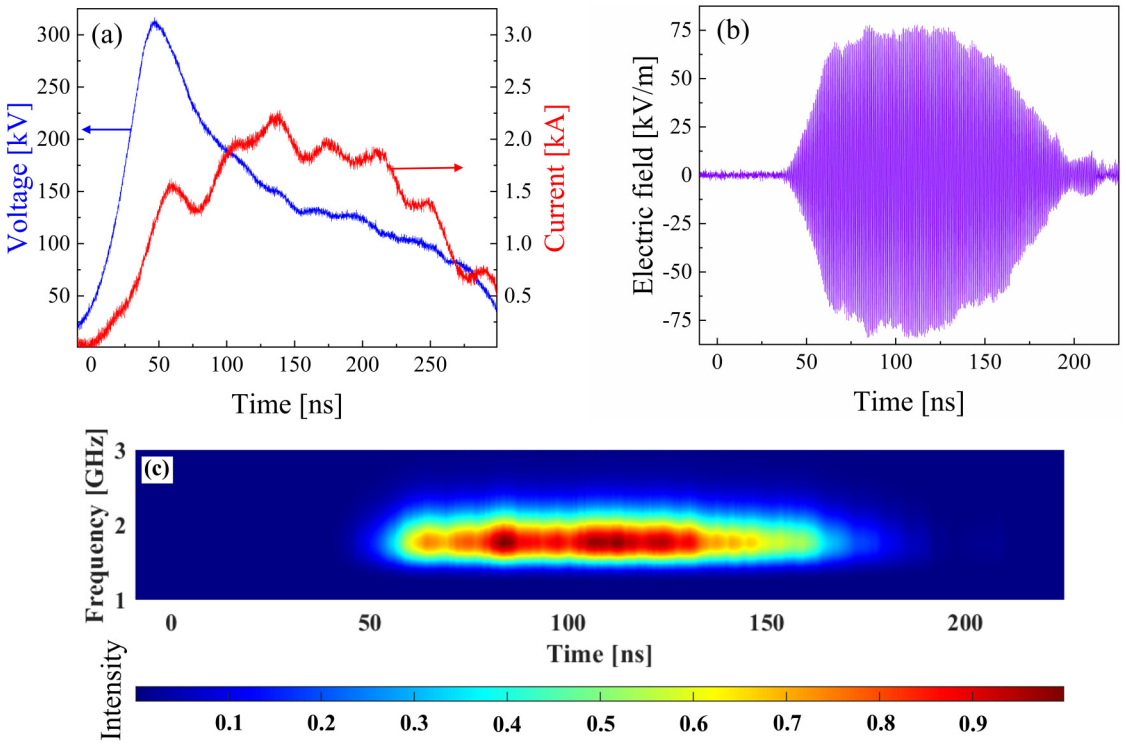

FIG. 2. (a) Waveforms of the voltage and RM current, (b) the electric field obtained by the D-dot with vertical polarization, and (c) time-frequency plot of the signal in (b); the colors represent the intensity (unitless) of the signal as a function of time and frequency and is normalized to the maximum intensity. Parameters: 60 mm long anode, 11.5 mm diameter cathode emitter, 6 mm diameter rod, $G = 15$ mm, $B_z = 0.32$ T, and $\varphi_{ch} = 2.6$ kV.

Similar dependencies as those shown in Fig. 4 were obtained for other LIA charging voltages and values of G.

The dependence of the voltage and current as a function of magnetic field for two values of the LIA charging voltage is shown in Fig. 5. Increasing the magnetic field leads to stronger electron magnetic insulation, which results in the decrease in the total current and increase in the voltage. The same behavior exists for a solid cathode fed RM, and dependencies similar to those seen in Fig. 5 were obtained for other values of G, φ_{ch} and for the 40 mm long anode.

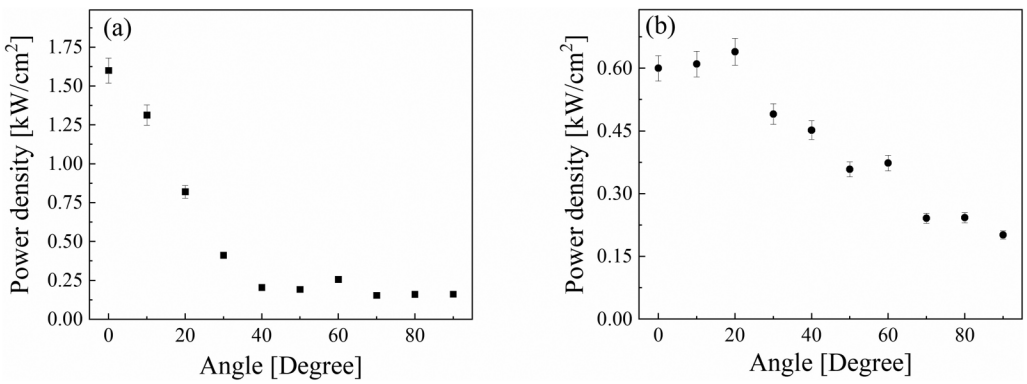

FIG. 3. Spatial distribution of the HPM power density at the distance of 190 cm from the antenna output (a) and without antenna from the RM output (b). Parameters: 60 mm long anode, 11.5 mm diameter cathode emitter, 6 mm diameter rod, $G = 30$ mm, $B_z = 0.3$ T, and $\varphi_{ch} = 2.6$ kV.

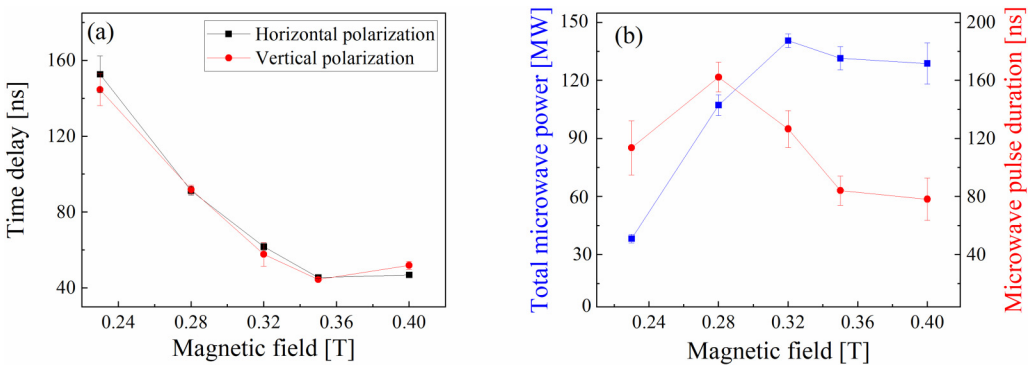

FIG. 4. (a) The time delay in the microwave generation and (b) the total radiated power and pulse duration vs the magnetic field. Parameters: 60 mm long anode, 11.5 mm diameter cathode emitter, 6 mm diameter rod, $G = 30$ mm, and $\varphi_{ch} = 2.6$ kV.

Decreasing the charging voltage of the LIA from 2.6 to 2.0 kV led to a decrease (~80%) in the HPM power, which is related to a decrease in the voltage (~20%) and in the RM current (~30%).

For a 40 mm long anode and different values of G, the main difference from the results obtained for the longer anode was that the HPM pulse duration was ≤110 ns and the frequency increases to 1.98 GHz. For a 40 mm long anode, the dependence of the total radiated HPM power on G is shown in Fig. 6(a) (11.5 mm diameter cathode emitter, $B_z = 0.4$ T, $\varphi_{ch} = 2.6$ kV). Similar dependencies were obtained for other values of B_z and φ_{ch}. One can see a non-monotonic dependence of the power with two well-defined maxima at 15 and 30 mm gaps at the same frequency of $f \approx 1.98$ GHz. In Fig. 6(b), the voltage and current amplitudes at the maximum of the radiated HPM electric field vs the gap G for the same conditions as in Fig. 6(a) are drawn. One can see the maxima of voltages and minima of currents also at the same values of G for which there are maxima in Fig. 6(a). We can only assume that the maxima in the radiated power at the maxima of voltages and minima of currents obtained at G = 15 and 30 mm can be related to the complex electron dynamics occurring in a split cathode fed RM studied recently [see Refs. 13, 18, 20, and 30]. Namely, these maxima obtained in radiated power can be related to some kind of synchronization between the longitudinal oscillating electrons with the RM mode and azimuthal drift of the bunches. However, when this synchronization is incomplete, this leads to less generated power, larger current toward the anode, and smaller voltage, keeping in mind that the LIA's constant impedance is ~100 Ω. Let us also note that an increase in G from 15 to 30 mm does not lead to decrease in the current as one would expect for common foil-less magnetically insulated diodes. This feature allows the split cathode fed RM operation at large G (≥30 mm) with no explosive emission plasma formation in the anode space during ≥300 ns.

For the same values of the parameters considered so far, that is, B_z, φ_{ch}, G, the anode length, and 6 mm diameter rod, increasing the emitter diameter from 11.5 to 16 mm resulted in a significant decrease (~25%) in the HPM total power. The latter can be related to a decrease in the initial potential energy of electrons in the anode interaction space for the larger diameter emitter. To confirm this hypothesis, the experiments were carried out for the same

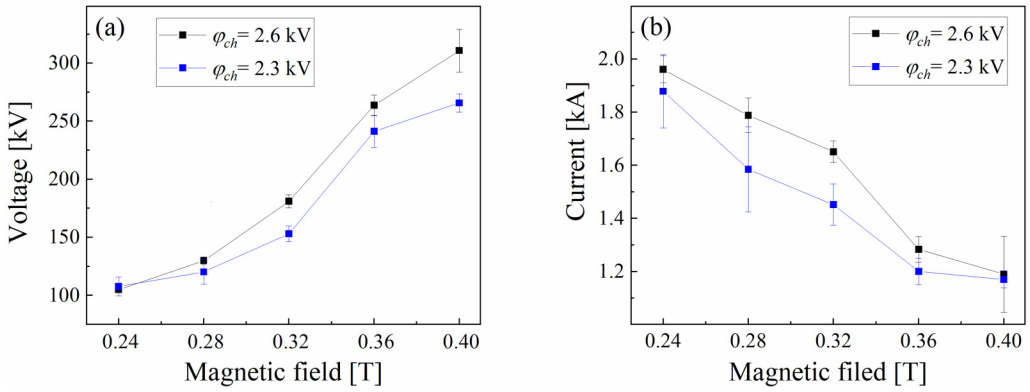

FIG. 5. The voltage (a) and current (b) at the maximum of the radiated HPM electric field vs the magnetic field for different charging voltages of the LIA. Parameters: 60 mm long anode, 11.5 mm diameter emitter, and $G = 15$ mm.

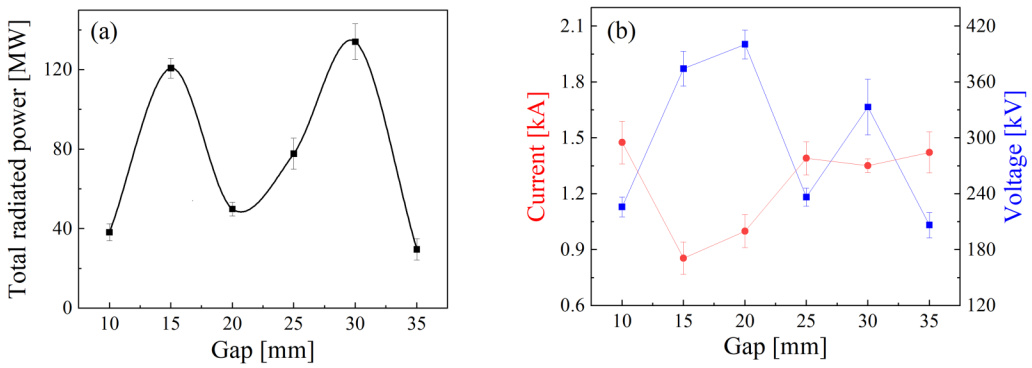

FIG. 6. The radiated microwave power (a) and the voltage and current at the maximum of the radiated HPM electric field (b) vs the gap length *G*. Parameters: 11.5 mm diameter emitter, 40 mm long anode, $B_z = 0.4$ T, and $\varphi_{ch} = 2.6$ kV.

parameters but with the emitter diameter of 11.5 mm, while the diameter of the rod was increased from 6 to 9 mm. For this case, electrons will oscillate inside the anode with potential energy closer the cathode potential than for the 6 mm diameter rod. Indeed, in these experiments, the measured HPM power increased by ∼15%.

Finally, when the reflector was replaced by a second cathode emitter, i.e., the split cathode consisted of two emitters at the same diameter and the same *G*. In these experiments, there was no change in the generated HPM pulse parameters and the LIA voltage and current compared to the results obtained with a single emitter for the same experimental conditions. This result showed that filling the potential well by oscillating electrons creating self-consistent space charge using a single emitter is sufficient.

B. Operation of the RM with a solid cathode

The solid carbon cathode was placed coaxially and centered with the anode center. Upstream and downstream reflectors were connected to the solid cathode by 6 mm diameter aluminum rods. The RM fed by this solid cathode was studied for $\varphi_{ch} = 2.0$–2.6 kV, magnetic fields, and $B_z = 0.23$–0.4 T and for different cathode diameters and lengths and anode lengths.

With a solid cathode, the RM also generates microwaves with radial polarization, i.e., with the vertical and horizontal polarizations having electric fields of almost the same amplitude in the both polarizations. However, in contrast to the split cathode case, the mode converter at the output of the RM cuts off the horizontally polarized component, but the amplitude of the electric field in the vertical polarization increases significantly (up to 2.5 times) with a corresponding increase in the HPM total power (from ∼140 to ∼240 MW). HPM generation starts at $B_z \geq 0.28$ T, which corresponds to the Hull limit, in contrast to the split cathode for which $B_z = 0.23$ T was sufficient for microwave generation.

The dependence of the LIA voltage and current at the maximal value of the HPM pulse amplitude on the magnetic field for two different LIA charging voltages is shown in Fig. 7. The behavior seen in Fig. 7 is similar to that in Fig. 5 and is the result of increasing magnetic insulation with increasing magnetic field.

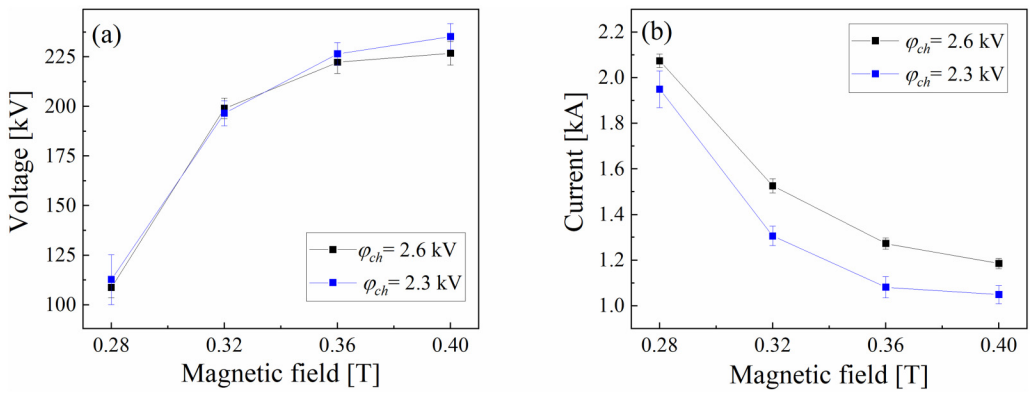

FIG. 7. Dependence of the voltage (a) and current (b) amplitudes measured at maximum of the HPM pulse amplitude on the magnetic field. Parameters: 16 mm diameter, 30 mm long cathode, and 40 mm long anode.

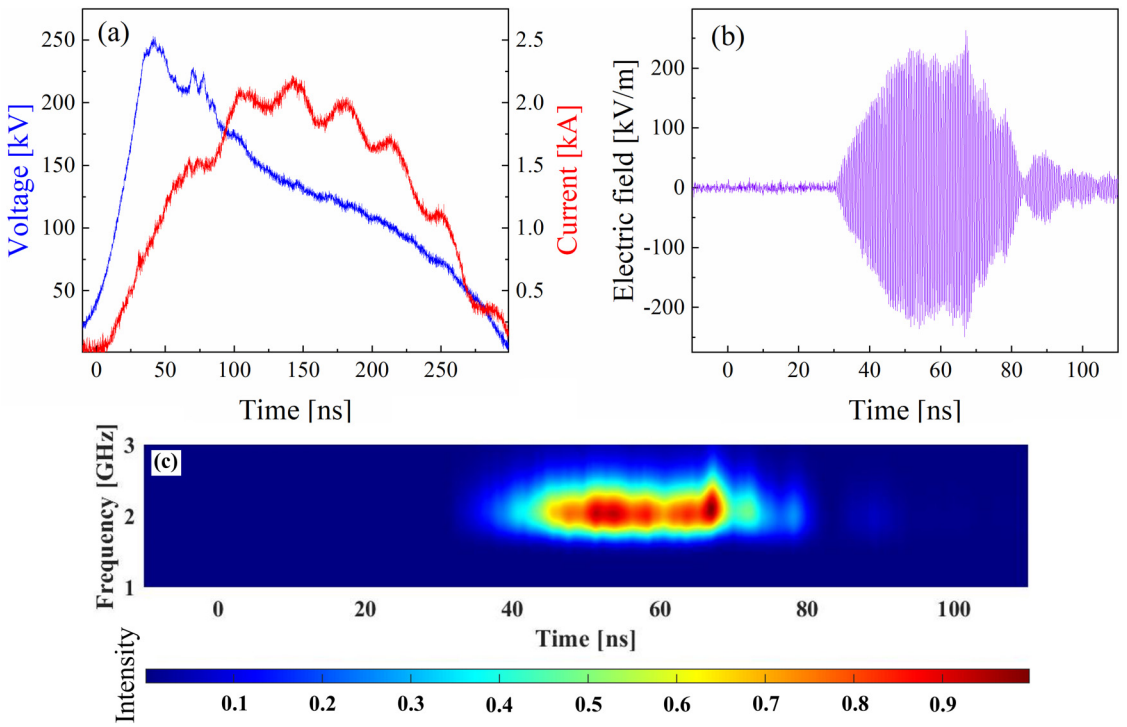

FIG. 8. Waveforms of the voltage and RM current (a), the HPM electric field measured by the D-dot probe with vertical polarization (b), and time-frequency analysis of the microwave pulse (c) [the color bar represents the same value as in Fig. 2(c)]. Parameters: 40 mm long anode, 16 mm diameter, 30 mm long solid cathode, $B_z = 0.35$ T, and $\varphi_{ch} = 2.6$ kV.

For the chosen solid cathode length, the result is that, as the magnetic field increases, the electron current is larger and the voltages is smaller compared to the split cathode case.

Typical waveforms of the RM voltage, φ_{LIA}, current I_{RM}, and microwave electric field measured by the D-dot placed 190 cm from the output of the antenna installed on the mode converter's downstream end and the time-frequency analysis of the electric field signal are shown in Fig. 8. These waveforms were obtained in the experiments with a 40 mm long anode, a 16 mm diameter, 30 mm long solid carbon cathode, and 6 mm diameter rods holding the emitter and two reflectors, $B_z = 0.35$ T and $\varphi_{ch} = 2.6$ kV. One can see in Fig. 8 that the microwave generation [Fig. 8(b)] starts with a time delay of $\tau \approx 35$ ns when the amplitude of the current reaches $I_{RM} = 0.8$ kA [Fig. 8(a)] and it continues ~45 ns with a frequency of f = 2.03 GHz, which is constant during the entire pulse. Figure 8(a) is very similar to Fig. 2(a), but the microwave pulse for the solid cathode is significantly shorter than the duration of the voltage pulse in contrast to the MW signal obtained with a split cathode [Fig. 2(b)]. Without the mode convertor, when the HPM power was ~140 MW, the pulse duration does not exceed 75 ns, indicating the presence of pulse shortening.

The spatial distribution of the HPM total power density was measured for the vertical and horizontal polarizations of the D-dot probe with and without the mode convertor. These measurements showed that, within measurement errors, the spatial distributions are almost the same as those obtained with the split cathode (see Fig. 3). Using these distributions, the total power of the HPM pulse obtained with the mode converter was calculated to be $P_{MW} = 240$ MW, which corresponds to an electronic efficiency $\eta = (P_{MW}/P_{LIA}) \times 100\% \approx 80\%$. Without the mode converter, the total radiated power does not exceed $P_{MW} = 140$ MW, that is, $\eta \approx 40\%$, similar to the values obtained for the split cathode fed RM. The near doubling of the power with the mode converter with the solid cathode was not expected. According to the results of our CST simulations, the mode converter should have only efficiently converted the TM_{01} mode to TE_{11}. Thus, a possible qualitative explanation for this is a partial reflection of the microwave power from the mode converter, leading to an increase in the power generated by the RM, similarly to an HPM amplifier. To confirm this assumption, we need more experiments and 3D Cartesian simulations, which we plan to perform in the near future. The power halving observed with the split cathode can be the result of the same power reflection. We have shown by simulations in previous publications[13,18] that the electron dynamics in a split cathode is complex and different from that with a solid cathode due to the axial oscillations of the electron cloud, which affects the azimuthal drifting of the electrons and the synchronization with the RM's mode. Thus, it is possible that a partial reflection of the HPM

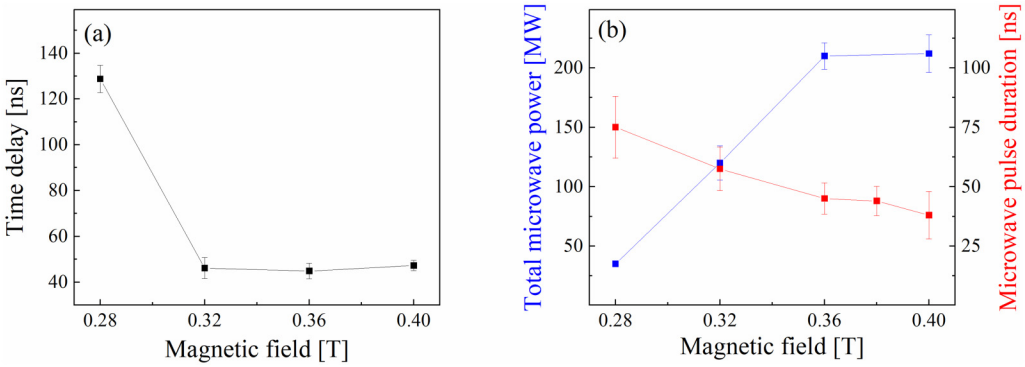

FIG. 9. (a) The time delay in the microwaves generation vs B_z (a) radiated power and pulse duration (b) vs the magnetic field. 40 mm long anode, 16 mm diameter and 30 mm long cathode emitter, 6 mm diameter reflector holder, and $\varphi_{ch} = 2.6$ kV.

power from the mode convertor, which leads to power doubling with the solid cathode causes power halving with the split cathode. This point, on its own, is interesting, and we need to investigate it in the future. For the solid cathode fed RM, such parameters as the time delay τ_d, the HPM pulse duration, and the HPM power also depend on the value of the magnetic field which we varied in the range 0.28–0.4 T. The results for a 16 mm diameter, 30 mm long solid cathode, 40 mm long anode, and 6 mm diameter rod, with the mode converter, are presented in Fig. 9. One can see [Fig. 9(a)] that the behavior is similar to that seen for a split cathode [Fig. 4(a)], and for increasing magnetic field, the time delay reduces to $\tau \approx 45$ ns. The HPM pulse duration is ~75 ns at 0.28 T and decreases with increasing magnetic field to ~38 ns for $B_z = 0.35$ T [Fig. 9(b)]. With the split cathode, the pulse duration decreased from values 90–120 to 80 ns when the magnetic field increased from 0.23–0.4 T [Fig. 4(b)]. Increasing the magnetic field leads to an increase in power and decrease in pulse duration. An example of this is seen in Fig. 7(b), and the results in Fig. 9(b), when compared to Fig. 4(b), indicate that pulse shortening exists for the solid cathode but not for the split cathode. Qualitatively similar dependencies as those seen in Fig. 9 were obtained for other geometrical parameters of the solid cathode fed RM and the LIA charging voltages.

Varying φ_{ch}, the diameter or length of the cathode effects the total power, but not the pulse duration, frequency, and the time delay. Similarly to the split cathode, for a solid cathode, decreasing φ_{ch} from 2.6 to 2.0 kV leads to a ~20% decrease in the HPM total power. An increase in the cathode diameter from 16 to 18.5 mm led to a ~ 30% decrease in the total power. Decreasing the cathode length from 30 to 17 mm led to a decrease in the total power by ~20%. The main differences in the parameters of the HPM pulse were obtained when the length of the anode was increased to 60 mm. For this case and the same solid cathode diameter (16 mm) and length (30 mm), the total power decreases from ~240 to ~170 MW and the frequency from 2.02 to 1.87 GHz. The duration of the HMP pulse was found to depend on the magnetic field value, and it decreases to ~70 ns at $B = 0.4$ T with the increase in the magnetic field. However, in the range $B = 0.28$–0.34 T, the pulse duration varied from pulse to pulse in the range 70–160 ns, probably the result of pulse shortening in some cases. For the solid explosive emission cathode, pulse shortening is the result of the radial expansion, instability, and non-uniformity of the cathode's explosive emission plasma. This leads to the violation of the synchronization between the azimuthally drifting electrons and the phase velocity of the electromagnetic mode of the magnetron. The application of the split cathode avoids this problem because the plasma forms outside the anode and remains outside until it reaches the anode. The axial expansion of the cathode plasma toward the anode can lead to HPM pulse shortening only after a time of the order of several hundreds of ns for an emitter–anode distance of a few cm. Note that the connecting rod does not emit plasma or electrons because it is screened by the charge of the oscillating electron cloud.[17–19]

IV. CONCLUSIONS

The experimental research presented in this article shows the high sensitivity of the HPM pulses generated by an S-band six-vane segmented axial output RM on geometrical, electrical parameters, and magnetic field values when either a split cathode or a solid explosive emission cathode is tested. It was shown that both cathodes can be applied successfully for the generation of HPM pulses of ~130 MW power and with similar electronic microwave generation efficiency (~40%) but without the mode converter. However, the RM's operation fed by the solid cathode is characterized by pulse shortening in contrast to the split cathode for which this effect is absent. The experiments with the solid cathode fed RM with the mode converter attached to it produced ~80% efficiency of ~240 MW power HPM pulses but only ~45 ns long. The reduction of the output power by the mode converter, when the split cathode is used, means that the electromagnetic mode produced at its output is not as designed by simulations.[18] Clarifying this point and additional optimization is required to increase the efficiency of the split cathode fed RM. We demonstrated yet again that the segmented anode allows using a much more compact μs-timescale magnetic field producing system, making it possible for the RM to operate repetitively.

ACKNOWLEDGMENTS

We are very grateful to Dr. I. Vintizenko and A. Mashenko for generous assistance in the repair and modification of the LIA, Dr. Y. Bliokh for fruitful discussions, and E. Flyat and S. Gleizer for their technical assistance in the experiments. At the Technion, this work was supported by Technion (Grant No. 2029541) and ONRG (Grant No. N62909-21-1-2006) and at the University of New Mexico by AFOSR (Grant No. FA9550-19-1-0225) and ONR (Grants Nos. N00014-19-1-2155 and N00014-23-1-2072).

AUTHOR DECLARATIONS

Conflict of Interest

The authors have no conflicts to disclose.

Author Contributions

O. Belozerov: Conceptualization (equal); Data curation (lead); Formal analysis (lead); Writing – original draft (equal); Writing – review & editing (equal). **Ya. E. Krasik:** Conceptualization (equal); Supervision (lead); Writing – original draft (equal); Writing – review & editing (equal). **J. G. Leopold:** Conceptualization (equal); Formal analysis (equal); Writing – review & editing (supporting). **S. Pavlov:** Conceptualization (equal); Data curation (supporting); Methodology (equal); Writing – original draft (supporting). **Y. Hadas:** Data curation (supporting); Methodology (supporting). **K. Kuchuk:** Formal analysis (supporting); Methodology (supporting). **E. Schamiloglu:** Formal analysis (equal); Writing – review & editing (equal).

DATA AVAILABILITY

The data that support the findings of this study are available from the corresponding author upon reasonable request.

REFERENCES

[1]G. Bekefi and T. J. Orzechowski, Phys. Rev. Lett. **37**, 379 (1976).
[2]J. Benford, J. A. Swegle, and E. Schamiloglu, *High Power Microwaves*, 3rd ed. (CRC Press, Boca Raton, FL, 2015).
[3]I. Vintizenko, *Linear Induction Accelerators for High-Power Microwave Devices* (CRC Press, 2018).
[4]D. Andreev, A. Kuskov, and E. Schamiloglu, Matter Radiat. Extremes **4**, 067201 (2019).
[5]D. Price, J. S. Levine, and J. N. Benford, IEEE Trans. Plasma Sci. **26**, 348 (1998).
[6]M. Fuks and E. Schamiloglu, Phys. Rev. Lett. **95**, 205101 (2005).
[7]M. I. Fuks, S. Prasad, and E. Schamiloglu, IEEE Trans. Plasma Sci. **44**, 1298 (2016).
[8]A. M. Ignatov and V. P. Tarakanov, Phys. Plasmas **1**, 741 (1994).
[9]M. Fuks and E. Schamiloglu, Phys. Rev. Lett. **122**, 224801 (2019).
[10]W. Li, J. Zhang, Z.-Q. Li, and J.-H. Yang, Phys. Plasmas **23**, 063109 (2016).
[11]A. J. Sandoval, "An experimental verification of A6 magnetron with permanent magnet," M.S. thesis (University of New Mexico, 2018), see https://digitalrepository.unm.edu/ece_etds/400/.
[12]Y. E. Krasik, J. G. Leopold, and U. Dai, IEEE Trans. Plasma Sci. **47**, 3997 (2019).
[13]J. G. Leopold, M. Siman Tov, S. Pavlov, V. Goloborodko, Y. E. Krasik, A. Kuskov, D. Andreev, and E. Schamiloglu, Appl. Phys. **130**, 034501 (2021).
[14]Y. Hadas, T. Kweller, A. Sayapin, Y. E. Krasik, and V. Bernshtam, J. Appl. Phys. **106**, 063306 (2009).
[15]S. P. Bugaev, V. I. Kanavez, V. I. Koshelev, and V. A. Cherepanov, *Relativistic Multi Wave Microwave Generators* (Siberian Division, Novosibirsk, 1991), pp. 81–94 (in Russian).
[16]S. Xu, L. Lei, F. Qin, and D. Wang, Phys. Plasmas **25**, 083301 (2018).
[17]J. G. Leopold, M. Siman Tov, S. Pavlov, V. Goloborodko, Y. E. Krasik, A. Kuskov, D. Andreev, and E. Schamiloglu, J. Appl. Phys. **130**, 034501 (2021).
[18]J. G. Leopold, Y. E. Krasik, Y. Hadas, and E. Schamiloglu, IEEE. Trans Electron Dev. **68**, 5227 (2021).
[19]Y. E. Krasik, J. G. Leopold, Y. Hadas, Y. Cao, S. Gleizer, E. Flyat, Y. P. Bliokh, D. Andreev, A. Kuskov, and E. Schamiloglu, J. Appl. Phys. **131**, 023301 (2022).
[20]Y. P. Bliokh, Y. E. Krasik, J. Leopold, and E. Schamiloglu, Phys. Plasmas **29**, 123901 (2022).
[21]J. G. Leopold, Y. Bliokh, Y. E. Krasik, A. Kuskov, and E. Schamiloglu, "Diocotron and electromagnetic modes in split-cathode fed relativistic smooth bore and six-vane magnetrons," Phys. Plasmas **30**, 013104 (2023).
[22]A. Sayapin, A. Levin, and Y. E. Krasik, IEEE Trans. Plasma Sci. **41**, 2506 (2013).
[23]A. Sayapin, A. Levin, and Y. E. Krasik, IEEE Trans. Plasma Sci. **41**, 3001 (2013).
[24]A. Sayapin, A. Levin, and Y. E. Krasik, IEEE Trans. Plasma Sci. **43**, 3827 (2015).
[25]A. Sayapin, U. Dai, and Y. E. Krasik, IEEE Trans. Plasma Sci. **45**, 229 (2017).
[26]A. Sayapin, U. Dai, and Y. E. Krasik, Appl. Phys. Lett. **111**, 233503 (2017).
[27]A. Chittora, Int. J. RF Microwave Comput. Aided Eng. **30**, e22317 (2020).
[28]See https://www.ansys.com/products/electronics/ansys-hfss for the Ansys HFSS software used for the simulation of the mode converter.
[29]Y. P. Raizer, *Gas Discharge Physics* (Springer-Verlag, Berlin, 1991).
[30]J. G. Leopold, Y. Bliokh, Y. E. Krasik, A. Kuskov, and E. Schamiloglu, Phys. Plasmas **30**, 013104 (2023).